Characterization of Neural Cells Derived from Reelin-deficient Schizophrenic Patient iPS Cells

2018

Nicole Roberts

CHARACTERIZATION OF NEURAL CELLS DERIVED FROM REELIN-DEFICIENT SCHIZOPHRENIC PATIENT IPS CELLS

by

NICOLE Y. ROBERTS
B.S. Biology & Psychology, Florida State University, 2010

A thesis submitted in partial fulfillment of the requirements
for the degree of Master of Science
in the Burnett School of Biomedical Science
in the College of Medicine
at the University of Central Florida
Orlando, Florida

Fall Term
2018

Major Professor: Kiminobu Sugaya

ABSTRACT

Reelin is a large, extracellular glycoprotein that binds to several membrane receptors on neural stem cells (HNSCs), neural progenitor cells (NPCs), and neuroblasts of mammals to direct their migration. Previously, our lab established the presence of Reelin increased migration of wild-type fetal-derived HNSC's, both *in vitro* and *in vivo*. In addition, we demonstrated that Reelin protein treatment also increases the formation of radial glia via Notch-1 signaling, *in vitro*. Radial glia are precursors to NPCs, as well as a scaffold for neuroblast migration during cortical lamination. Reelin has long been associated with Schizophrenia (SZ). Because post-mortem brains are limited to describing the end-point of the disease, heterozygous haplodeficient Reelin knock-out (*Reeler)* mice are used to model developmental aspects of SZ *in vivo*. However, SZ is a complex, polyfactoral disease with a myriad of dysfunctional pathways that may have unforeseen effects on Reelin signaling. K. Brennand et al. (2014) reported low Reelin mRNA expression and cellular characteristics mirroring the *Reeler* mouse in induced pluripotent stem (iPS) cell-derived NPCs and neurons from living SZ patients. Building upon this and our work with stem cells, here we consider Reelin's effects on migration of Reelin-deficient iPS cell-derived NPCs. Reelin treatment of consists of secreted Reelin from transfected human embryonic kidney 293 cells (HEK 293) with the pCRL RELN gene-containing plasmid created by G. D'Arcangelo (1997) and given to us by T. Curran. Using the metric of cellular migration, this is the first time it have been shown that SZ iNPCs are capable of receiving and reacting to extracellular Reelin. Due to our validation of this model, further work using iPS cell-derived neural cells can confidently be used for future disease modeling and drug discovery of Reelin-deficient SZ.

ACKNOWLEDGMENTS

A special thank you to Dr. Steven Ebert for his feedback and insight; to Dr. Michal Masternak for generously agreeing to be in my committee for the home stretch; to Dr. Alvaro Estevez for his encouragement even during his transition away from UCF; to Dr. Ravi Nadimpalli and Manjusha Vaidya in the Sugaya Lab for their help in the lab; to Dr. Saleh Naser and Lisa Vaughn for their administrative guidance and keeping me on track, Kristen Skruber for being my academic role model and graduate student advice-giver; to my peers in the program (specifically Kritika Kedarinath, Candace Fox, Georgili Nobleza, and Levi Adams) for commiserating and helping me problem-solve; and most importantly, to Dr. Kiminobu Sugaya for being a kind mentor and teaching me how to learn from my failures as much as my successes.

TABLE OF CONTENTS

LIST OF FIGURES

LIST OF ACRONYMS AND ABBREVIATIONS

µL	Microliter
µM	Micromolar
µm	Micrometer
AB/AM	Antibacterial/antimycotic
AMPAR	α-amino-3-hydroxy-5-methyl-4-isoxazolepropionic acid receptor
ApoER2	Apolipoprotein E receptor 2
BamHI	*Bacillus* amyloliquefaciens H I endonuclease
BCA	Bicinchoninic acid
bFGF	Basic fibroblast growth factor
bp	Base pairs
BSA	Bovine serum albumin
Ctrl	Control

Dab1	Disabled 1 protein
DMSO	Dimethylsulfoxide
DMEM	Dulbecco's Modified Eagle's Medium
EDTA	Ethylenediaminetetraacetic acid
EGF	Epidermal growth factor
EtOH	Ethanol
E. coli	*Escherichia* coli
EcoRI	E. coli RY13 endonuclease
FBS	Fetal bovine serum
fHNSC	Fetal brain-derived human neural stem cell
g	Gram
GABA	γ-aminobutyric acid
GAPDH	Glyceraldehyde 3-phosphate dehydrogenase
hr	Hour

HCl	Hydrochloric acid
HEK	Human embryonic kidney
HNSC	Human neural stem cell
HRM	Heterozygous/haplodeficient *reeler* mouse
HRP	Horseradish peroxidase
IgG H&L	Immunoglobulin G heavy and light chain
iHNSC	Induced pluripotent stem cell-derived human neural stem cell
iNPC	Induced pluripotent stem cell-derived neural progenitor cell
ICC	Immunocytochemistry
iPS cell	Induced pluripotent stem cell
IZ	Intermediate zone
kb	Kilobase pairs
KSR	Knockout Serum Replacement

L	Liter
LDS	Lithium dodecyl sulfate
LTP	Long-term potentiation
M	Molarity (moles/L)
MEF	Maurine embryonic fibroblast
mg	Milligram
min	Minute
mL	Milliliter
mM	Millimolar
mmol	Millimole
MOPS	(3-(N-morpholino)propanesulfonic acid)
MARGINAL ZONE	Marginal zone
NEAA	Non-essential amino acids

nm	Nanometer
NMDAR	N-methyl-D-aspartate receptor
NPC	Neural progenitor cell
NSC	Neural stem cell
NT2	Ntera-2
O/N	Overnight
PAGE	Polyacrylamide gel electrophoresis
pEGFP	Enhanced green fluorescent protein-expressing plasmid
PVDF	Polyvinyldiene difluride
rcf	Relative centrifugal force
reeler	Reelin knockout mouse model
RELN	Reelin gene
RIPA	Radio-Immunoprecipitation Assay

RT	Room temperature
rt-PCR	Reverse transcriptase-polymerase chain reaction
SDS	Sodium dodecyl sulfate
SZ	Subventricular Zone
TBS-T	Tris buffer saline with tween 20
TGF-β	Transforming growth factor-β
UV	Ultraviolet
VLDLR	Very low density lipoprotein receptor
VZ	Ventricular zone
wt	Wild type

I. INTRODUCTION

From commencement to completion, Reelin guides the development of the cortex, cerebellum, and hippocampus via a ballet of intertwining pathways that scientists are still discovering today. Previously our lab demonstrated increased formation of radial glia (progenitor cells that provide a scaffold for migrating neurons) via Notch-1 signaling in wild type fetal-derived human neural progenitor cells as a direct result of Reelin protein treatment.[1] Kim et al. (2002) determined Reelin secretion is integral to the migration of NPCs, both *in vitro* and in the heterozygous Reelin-deficient (*Reeler)* mouse model.[2] Reelin deficiency was established to be responsible for the delayed dendritic growth in *Reeler* mice.[3] Additionally, Reelin was shown to promote long-term potentiation (LTP) by altering glutamate receptor composition in the membrane.[4] As evidenced by the both *in vitro* and *in vivo* experiments, disruptions in the Reelin signaling pathway lead to deviations in the standard structure of the cortex and long-term changes in neuronal development and maturation, as seen in Schizophrenia (SZ).

Reelin is a 388 kDa glycoprotein secreted into the extracellular matrix during mammalian brain development by specialized neurons called "Cajal-Retzius cells" located in the marginal zone of the cortex and the outer molecular layer of the dentate gyrus in the hippocampus.[5, 6] In adults, Reelin is secreted by: 1) a subset of γ-aminobutyric acid (GABA)ergic interneurons in the cortex (specifically horizontal cells in layer I, bitufted neurons in layers II-V, and Martinotti cells in layers II-VI), 2) CA1 GABAergic interneurons in the hippocampus, 3) glutamatergic granular cells in the cerebellum, and 4) neurons of the entorhino-hippocampal pathway that guide migrating neural stem cells to the olfactory bulb [4, 6, 7] Reelin binds to α3/β1 integrin, very low density lipoprotein

receptor (VLDLR), and apolipoprotein E receptor 2 (ApoER2) complexes on the target cell membrane. Neural stem cells (NSCs), radial glia, neural progenitor cells (NPCs), neuroblasts, and mature interneurons – specifically glutamatergic Purkinji cells in the cortex, GABAergic chandelier and basket interneurons in the cortex, glutamatergic CA1 pyramidal neurons in the hippocampus, and GABAergic interneurons in the cerebellum possess the protein machinery to respond to Reelin.[2, 5, 7-9] Radial glia are progenitor cells that give rise to NPCs, as well as provide the scaffold upon which the NPCs migrate.[1, 10, 11] The activation of VLDLR/ApoER2 recruits a cytosolic adaptor protein, Disabled 1 (Dab1), which binds to the NPxY motifs at the tail of the receptors.[12] Fyn and Src – SRC-family kinases (SFK) – phosphorylate and activate Dab1 initiating the majority of the Reelin pathway signal transduction.[8] As seen in **Figure 1**, the effect on the cell varies and depends on the target cell type: NSC cultures respond with increased radial glia formation[1]; NPCs mature from multipolar cells to bipolar cells [13]; immature neurons react by extending their apical process to the marginal zone[14], then releasing the radial glia scaffold and tangentially migrating[15, 16]; and mature neurons will increase the total number, length, and branching of dendrites[3], as well as form more dendritic spines [17]. Furthermore, glutamatergic neurons experience an improvement in synaptic plasticity due to increased N-Methyl-D-Aspartate Receptor (NMDAR) subunit NR2B and α-amino-3-hydroxy-5-Methyl-4-isoxazolePropionic Acid Receptors (AMPAR) in the synaptic cleft in the presence of Reelin.[9] Phosphorylation of Dab1 leads to its subsequent ubiquitination, a negative feedback that leads to a decrease in total protein levels.[8]

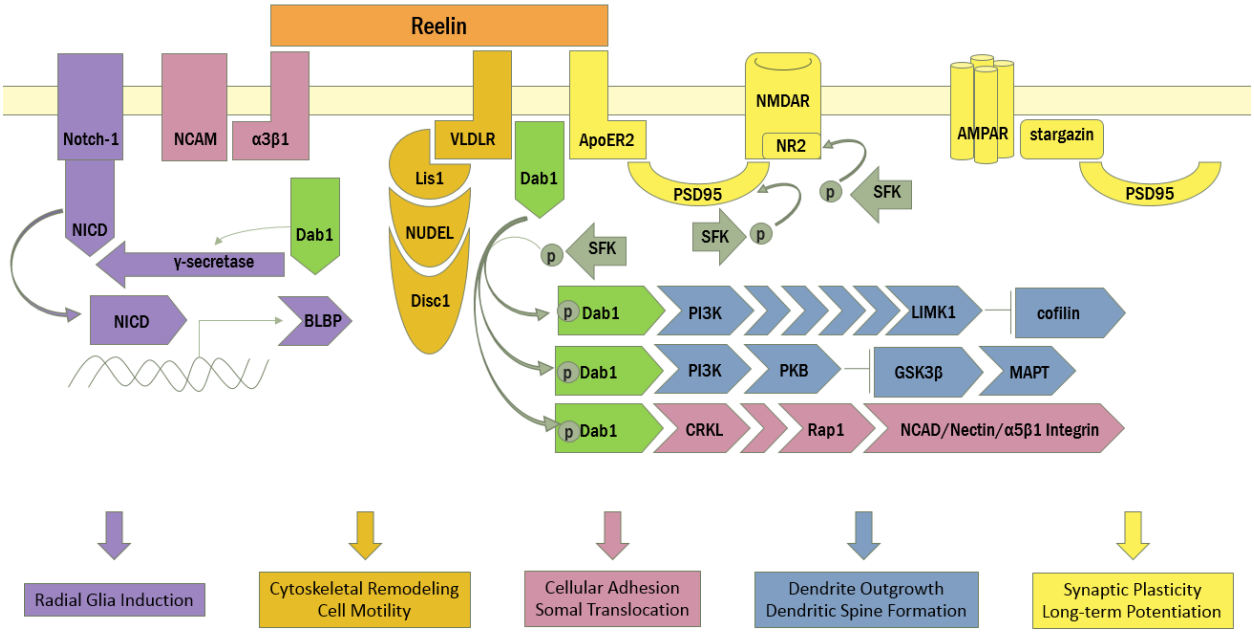

Figure 1. Reelin Molecular Pathway. NICD: Notch-1 Intracellular Domain, BLBP: Brain Lipid-Binding Protein, NCAM: Neural Cell Adhesion Molecule, α3β1: α3β1 integrin, Dab1: DisABled 1, VLDLR: Very Low Density Lipoprotein Receptor, NUDEL: NUclear Distribution protein nudE-like, Disc-1: Disrupted In Schizophrenia 1, ApoER2: Apolipoprotein E Receptor 2, PSD95: Post-Synaptic Density 95, NMDAR: N-Methyl-D-Aspartate Receptor, NR2: NMDAR subtype 2, AMPAR: α-amino-3-hydroxy-5-Methyl-4-isoxazolePropionic Acid Receptor, SFK: Src-Family Kinase, PI3K: PhosphoInositide 3-Kinase, LIMK1: Lin11/Isl-1/Mec-3 Kinase, PKB: Protein Kinase B, GSK3β: Glycogen synthase kinase 3 β, MAPT: Microtubule-Associated Protein – Tau, CRKL: CT10 Regulator of Kinase-Like, Rap1: Ras-proximate-1, NCAD: Neural CADherin

During typical cortical lamination, Cajal-Retzius cells in the marginal zone secrete Reelin forming a concentration gradient – with the highest concentration of Reelin at the marginal zone and the lowest at the ventricular zone.[6, 18] When Reelin reaches the ventricular zone, it prompts NSCs to form radial glia creating a scaffold that stretches all the way to the marginal zone. The radial glia asymmetrically divide producing NPCs. [18] Reelin promotes the NPC differentiation into bipolar immature neurons, as well at their apical process extension and anchoring to the marginal zone.[14]

The immature neurons then migrate up the radial glia scaffold toward the marginal zone.[18] According to the "detach and go" model, when these immature neurons reach a high enough concentration of Reelin, they stop and separate from the radial glia scaffold, then begin to tangentially migrate using the anchored process as a positional guide and forming the subplate.[18, 19] The next layer of migrating cells invade the subplate and then similarly migrate to their final destination, as dictated by the Reelin concentration gradient. These neurons will differentiate into pyramidal or horizontal neurons that form Layer VI of the cortex.[18] This process continues creating the distinctive inside-out, organized stratification of the six laminae in the cortex of a normal brain, as seen in **Figure 2**.

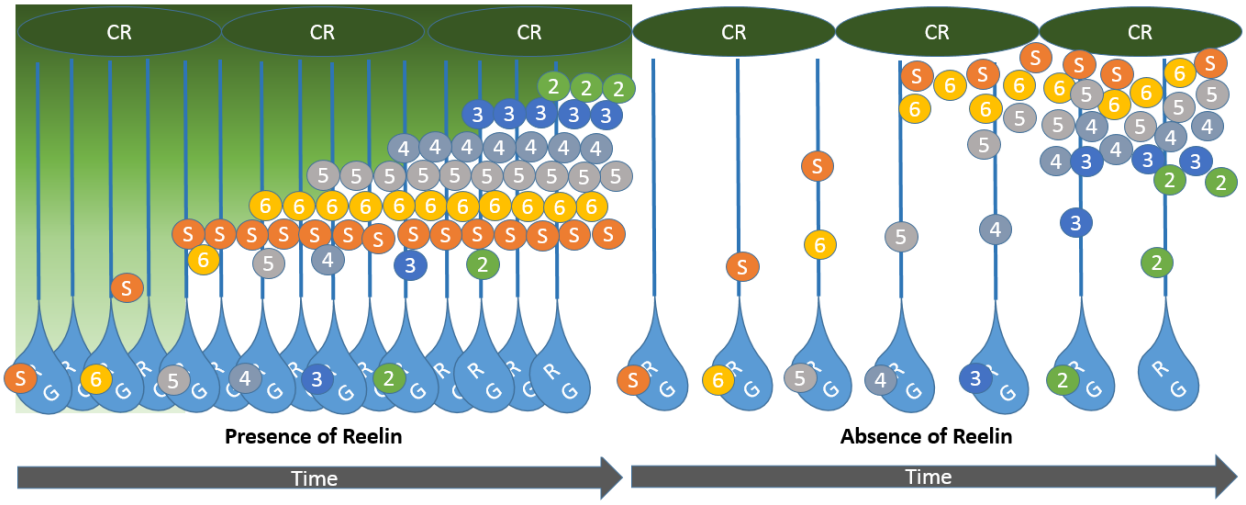

Figure 2. Lamination of the Cortex in the Presence and Absence of Reelin. Green-to-white gradient: Reelin concentration gradient, CR: Cajal-Retiez cells, RG: Radial Glia, S: neuronal cells to form the Subplate, 6: neuronal cells to form Layer VI, 5: neuronal cells to form Layer V, 4: neuronal cells to form Layer IV, 3: neuronal cells to form Layer III, 2: neuronal cells to form Layer II.

In postnatal mammalians, Reelin is responsible for continual migration of NSCs from the subventricular zone and dentate gyrus of the hippocampus to the olfactory bulb.[20]. During neuronal maturation in the first few weeks after birth, Reelin activates the pathways directly involved in the formation of dendrites and synapses, including dendritic spines and postsynaptic densities.[17, 21, 22] The high number of dendritic arborizations and dendritic spines allows for the adaptive ability of neurons to transduce novel information from the environment.[8, 17, 22, 23] It has been noted that Reelin is also capable of facilitating the maturation of glutamatergic synapses and enhancing long-term potentiation (LTP) via NMDAR subunit NR2 phosphorylation and increased AMPAR insertion into the membrane.[9, 24, 25] Overall, it appears that Reelin is required for normal maintenance of synaptic function, connectivity, and plasticity.

When Reelin is absent, as in the case of the homozygous Reelin knockout (*Reeler*) mouse, the cortex laminae are in the reverse, outside-in order with a 'superplate' consisting of the subplate and Layer VI combined with the marginal zone. The superplate forms because the neuroblasts are able to migrate radially, but do not receive a signal to extend their apical process, detach from the radial glia, or migrate tangentially to form the appropriate layer.[3, 19] The disorganized fashion of the *Reeler* cortex suggests that neuronal fates are determined by the timing of their conception and not their final location.[19] In homozygous *Reeler* mice, cerebellar hypoplasia and laminae defects causes ataxia and their characteristic "reeling" gait.[5] Additionally, *Reeler* mice suffer from learning deficits due to reduced LTP, altered dendritic spine morphology, and fewer total number of dendritic spines.[26, 27] Complete absence of Reelin in humans is a severe developmental disorder with a life expectancy of 10yrs called Lissencephaly, literally meaning "smooth brain".[28]

However, both humans and mice can be haplodeficient, due to either inheriting a gene mutation on a single allele (heterozygous) or a partial silencing of the wild type gene via methylation.[21] One study suggests that prenatal stress alone is enough to methylate the Reelin promoter and down-regulate its expression.[29] Others demonstrate reduced Reelin expression in offspring due to maternal infection and inflammation during pregnancy.[30-32] The cortex of adult heterozygous Reeler mice maintains its inside-out organization and appears phenotypically normal. Furthermore, these animals do not experience ataxia and exhibit a normal gait.[6] However, heterozygous *Reeler* mice display a delay in apical process formation during corticogenesis[3] and the pups have fewer total dendritic spines in the cortex and hippocampus.[25, 27, 33] The subtle temporal disturbances in development result in impairments in the formation and maturation of synapses, increased neuronal packing density, decreased LTP, and diminished GABAergic signaling[14, 25, 32, 34], which in turn lead to behavioral and cognitive abnormalities similar to neuropsychiatric disorders, such as SZ[14]. Mice and rats with either functionally less total Reelin protein or impaired Reelin pathway activation present with: hyperactivity[29, 35-37], inability to inhibit startle response after a prepulse warning[30, 34, 38], hyperanxiety[29, 30] or hypoanxiety[35, 37, 39], reduced sociability[30, 35, 39], and even impaired memory under some conditions. [25, 29, 31, 35, 37]

Although SZ is polyfactoral, impairments in the Reelin pathway have been consistently implicated. Researchers have reported methylations[21, 40-42] and reoccurring polymorphisms[43-48] of the Reelin gene in post-mortem SZ patient brains, as well as decreased Reelin mRNA and protein expression throughout the cortex, hippocampus, and cerebellum.[48-52] Abnormal density and aberrant location of interstitial white matter neurons[53] and Layer II pre-alpha cell clusters[54] found in the post-mortem cortex of SZ patients suggests deviations in normal migration due to insufficient Reelin.

Layer III neurons exhibited decreased dendritic spine density and reduced neuropil density, thus increasing cell packing density as compared to the control.[55, 56] *In vitro*, reelin-deficient SZ patient iPS cell-derived mature neurons also demonstrate fewer, shorter, and less complex dendrites, as well as weakened interconnectivity as compared to the wild type control.[57] The same cells were recorded to have deficits in migration as NPCs.[58]

Human iPS cells have often been chosen as an *in vitro* alternative in the past due to their ability to replicate human pathways that may be altered in animal cells. Numerous studies on iPS cells have demonstrated the capabilities of this model to parallel the processes that occur inside both wild type and disease-affected cells *in vivo*.[10, 11, 57, 59-64] Due to the nature of humans and their anatomy, patient brain tissue samples can only be obtained, ethically, post-mortem. These samples are not only difficult to acquire, but provide only a characterization of the endpoint stage of disease. In addition, schizophrenic patient post-mortem samples have been characterized by proteomics and transcriptomics, however the act of neuroblast migration cannot be observed nor treated with dead tissue.[58, 61] Because of the limitations on experimental research in post-mortem samples, disease modeling and drug discovery are often performed in an animal model. However, animal models are restricted by non-human physiology and cellular signaling, as well as the inability to communicate with humans when experiencing psychological symptoms of disease. In the case of SZ, *reeler* mice are a model that provides only a single pathway deficiency, while SZ is a multi-factorial disorder.[50, 62, 65-71] However, iPS cells from a live patient have the capability to demonstrate the specific phenotypic and molecular changes due to Reelin deficiency at any stage of development within a disease that may contain multiple genetic defects. And yet, there have been no studies have been conducted concerning the relationship between SZ iPS cell-derived

HNSC/NPC (iHNSC/iNPC) characteristics and Reelin. Using the metric of migration, we show that SZ NPCs dysfunction can be rescued with Reelin.

II. MATERIALS & METHODS

2.1 Cell Culture.

iPS Cell Culture: Reelin-deficient fibroblast-derived SZ iPS cells were acquired via the Coriell Repository (GM23760B). Thawed at passage 25, these cells were originally grown on murine embryonic fibroblast (Gibco, A24903) feeder layer following Coriell manual instructions in sterile, tissue-culture treated T75 flasks (Corning, 430641). Stem cell media contained: 20% Knockout Serum Replacement (KSR) (Gibco, 10828028), 1% MEM Non-essential amino acids (NEAA) (Gibco, 11140050), 1:1,000 β-mercaptoethanol/2-mercaptoethanol (Gibco, 21985023), 50 ng/mL recombinant basic Fibroblast Growth Factor (bFGF) (R&D Systems, 233-FB-01M) in Dulbecco's Modified Eagle's Medium (DMEM)/F12 with L-glutamine, HEPES, and phenol red (Gibco, 11330032). Thawing required the addition of 10uM ROCK inhibitor y-27632 (Sigma, Y0503-1MG). After 3 passages with 1 mg/mL collagenase, cells were transferred to the mTeSR 1 system (STEMCELL, 05850) following product manual protocol. Passaging was performed with ReLeSR (STEMCELL, 05872) as per product manual protocol.

Neural Induction: After 5 passages in mTeSR, cells were transferred to neural induction medium in a sterile T75 suspension flask (Thermo Scientific, 156800). Neural induction medium consisted of 20% KSR, 10% CTS Glutamax I (Gibco, A1286001), 1% non-essential amino acids, 1:1000 β-mercaptoethanol/2-mercaptoethanol, 400 ng/mL recombinant human Noggin (Gibco, PHC1506), 10 uM SB431542/ Transforming growth factor-β (TGF-β) inhibitor (Sigma, S4317-5MG), 2 ug/mL heparin sodium (Sagent Pharmaceuticals, NDC#25021 402-10), 20 ng/mL recombinant

bFGF in Neurobasal Medium (Gibco, 21103049). Embryoid bodies were cultured in neural induction media for 5 days, then transferred to HNSC media.

iHNSC Culture: SZ iPS cell-derived HNSCs (iHNSCs) were grown in sterile T75 suspension flasks (Thermo Scientific, 156800) with HNSC medium: 0.50 U/mL heparin sodium (Sagent Pharmaceuticals, NDC#25021 402-10), 20 ng/mL recombinant human epidermal growth factor (EGF) (R&D Systems, 236-EG-01M), 20 ng/mL recombinant bFGF (R&D Systems, 233-FB-01M), 2% B27 (Gibco, 17504044), 5% antibacterial/antimycotic (AB/AM) (Gibco, 15240062) in DMEM/F12 with L-glutamine, HEPES, and phenol red (Gibco, 11330032) . SZ iHNSCs had a 50:50 media change once per week, or earlier if phenol red indicator suggested high amount of growth. Depending on the size of the colonies, SZ iHNSCs were mechanically passaged with a scalpel or enzymatically passaged with StemPro Accutase Cell Dissociation Reagent (Gibco, A1110501) following product protocol. Passaging and splitting of flasks occurred once per week or less, depending on the size and number of colonies.

Differentiated iHNSC Culture: SZ iNPCs and neurons were all differentiated and maintained in tissue-culture treated flasks or plates, depending on the experiment, in Ntera-2 (NT2) medium: 10% fetal bovine serum (FBS) (Gibco, 16000044) and 5% AB/AM (Gibco, 15240062) in DMEM/F12 with L-Glutamine, HEPES, and phenol red (Gibco, 11330032). Cells were fed twice a week, depending on the color of the phenol indicator.

HEK293 cells Culture: Human embryonic kidney (HEK)-293 cells were maintained in sterile, tissue-culture treated T75 flasks (Corning, 430641) in 10% FBS (Gibco, 16000044), 5% AB/AM (Gibco, 15240062) in DMEM with glucose, L-Glutamine, sodium pyruvate, and phenol red

(Corning, 10-013-CM). Cells were passaged with Trypsin-EDTA (Ethylenediaminetetraacetic acid) (0.25%) with phenol red (Gibco, 25200056) once per week.

2.2 SZ Neural Differentiation Confirmation.

iHNSC and iNPC Confirmation via Reverse Transcriptase-Polymerase Chain Reaction (rt-PCR): RNA was isolated from all cells samples using TRIzol Reagent (Invitrogen, 15596018), Chloroform (Fisher, BP1145-1), Isopropanol (Sigma, 34863), 75% Ethanol (Sigma, E7023-500ML), and RNase-free water (Cellgro, 46-000-CM), according to the TRIzol product manual. Isolated RNA was converted to cDNA using the SuperScript III First Strand Synthesis System (Invitrogen, 18080051). PCR amplification was done on an Eppendorf Mastercycler epgradient S thermocycler and then run on an agarose gel. PCR for GAPDH, CD133 (a marker for stem cells), and beta-III-tubulin (a marker for neuronal cells) was performed with the AmpliTaq Gold 360 DNA polymerase kit following their 50 uL reaction protocol. The PCR product was run in a 2% E-gel with SYBR SAFE (Invitrogen, G521802), as per product manual protocol. The DNA ladder was 100 bp GeneRuler Plus (Fermentas, SM0321).

Forward primer for GAPDH: ATGTCGTGGAGTCTACTGGTC.

Reverse primer for GAPDH: AGAGTGGGAGTTGCTGTTGAA.

Forward primer for CD133: CAGAGTACAACGCCAAACCA.

Reverse primer for CD133: AAATCACGATGAGGGTCAGC.

Thermocycler settings: 7 minutes at 95°C; 30 cycles of 25 seconds at 95°C, 30 seconds at 52°C, 45 seconds at 72°C; then 7 minutes of 72°C.

Forward primer for beta-III-tubulin: AAGCCGCAGTGTCTAAACC.

Reverse primer for beta-III-tubulin: CCCGAAATATAAACACAAA.

Thermocycler settings: 7 minutes at 95°C; 30 cycles of 25 seconds at 95°C, 30 seconds at 42°C, 30 seconds at 72°C; then 7 minutes of 72°C.

iNPC Confirmation via Immunocytochemistry/Immunofluorescence (ICC/IF): SZ iHNSCs were plated on a 12-well plate for 10 days in NT2 medium to differentiate. Samples were fixed and permeablized with 100% methanol (Sigma, 34860-1L) at -20°C for 25 mins. Blocking and dilution was performed with 5% BSA in Tris-Buffered Saline with 0.2% Tween (TBS-T). Rabbit-host anti-Beta-III-Tubulin (BIIIT) antibodies (abcam, ab18207) at 1:2000 and mouse-host anti-Glial Fibrillary Associated Protein (GFAP) antibodies (abcam, ab190288) at 1:1000 were co-incubated overnight (O/N) at 4°C. Fluorescein Isothiocyanate (FITC)-conjugated donkey-host anti-mouse antibodies (Jackson, 715-095-150) and Tetramethylrhodamine (TRITC)-conjugated donkey host anti-rabbit antibodies (Jackson, 711-025-152) at 1:100 were incubated one hr at room temperature (RT) in a humidified chamber. Vectashield anti-fade mounting medium with DAPI (4',6-diamidino-2-phenylindole, dihydrochloride) (Vector Laboratories, H-1200) was applied and the cells were imaged with a Zeiss AX10 fluorescent microscope.

2.3 Reelin Production and Concentration.

Plasmids: The full length Reelin-expressing pCRL plasmid was constructed by Gabriella D'Archangelo (1995) and given to our lab by Tom Curran from St. Jude Children's Research Hospital, Memphis Tennessee.[6] The pCRL, pCDNA3.1 (Invitrogen, V79020), and pEGFP (plasmid enhanced green fluorescent protein) (Invitrogen) plasmids were amplified via One Shot

TOP10 Chemically Competent *Escherichia* (*E.*) coli (Thermo Scientific, C404003) LB broth (Fisher, BP1426-500) with 0.1% Ampicillin (Gibco, 11593027) or kanamycin (Gibco, 11815024), following product protocol for transformation. Plasmids were isolated using QIAprep Spin Miniprep kit (Qiagen, 27104).

pCRL Confirmation via Enyzme Digestion: pCRL plasmid was verified via Fast Digest Restriction Enzyme Digest for BamHI (*Bacillus* amyloliquefaciens H) (Thermo Scientific, FD0054) and EcoRI (*E.* coli RY13) (Thermo Scientific, FD0274) endonuclease enzyme cut sites, using the given manual protocol.

RELN Sequence Confirmation via PCR: RELN sequence was confirmed intact on the pCRL plasmid via PCR using MyTaq Red Mix (Bioline, BIO-25043). Gels were made at 2% agarose (Benchmark Scientific, A1705) with SYBR SAFE (Invitrogen, S33102). The O'GeneRuler 1 Kb Plus (Thermo Scientific, SM1343) DNA ladder was used as the standard.

Forward primer for *RELN*: TGAGTTCTCGGGAGGAGAGA.

Reverse primer for *RELN*: GGCACTTCCCATGAAGAAAA.

Thermocycler settings: 10 minutes at 95°C, then 40 cycles of 15 seconds at 95°C and 1 minute at 60°C as per Ovadia and Shifman (2011).[48]

HEK293 Cell Transfection: HEK293 cells were transfected with pCRL and pCDNA 3.1 plasmids in sterile, tissue-culture treated T150 flasks (Corning, 355001) with Lipofectamine 2000 (Invitrogen, 11668027) in OptiMEM (Gibco, 31985070) using the product sheet scaled up appropriately. HEK293 cells were allowed to incubate in the transfection medium for 72 hr. Media were collected after 1 week and concentrated via centrifugation using a 100K MWCO protein

concentrator (Pierce, 88532). Reelin protein presence was validated first via dot blot, then with western blot.

Reelin Secretion Confirmation via Dot Blot: Serial dilutions of transfected-HEK293 cell-conditioned media (1:1, 1:5, 1:125, 1:625, 1:3125) were loaded into the wells of a 96-well Bio-Dot dot blotter (Bio-Rad) on a nitrocellulose membrane (Bio-Rad, 162-0252) following the Bio-Dot protocol. Membrane was blocked with 5% milk in TBS-T (tris buffer saline with 0.1% tween 20) for one hr at RT, incubated in 1:1,000 Mouse Anti-Reelin antibody [G10] (abcam, ab78540) for two hr, then incubated in 1:10,000 Goat Anti-Mouse IgG H&L(immunoglobulin G heavy and light chain) horseradish peroxidase (HRP)-conjugated antibody (abcam, ab6789) for one hr at RT. Imaged with ECL substrate (Thermo Fisher, 32132) on a Kodak Image Station 4000mm PRO imager.

Reelin Concentration: Whole media from transfected-HEK cells was collected and frozen at -80*C every 3 days for one month after transfection. Media was then thawed and concentrated in 20 mL batches via the 100K MWCO Pierce Protein Concentrator (Thermo Fisher, 88532) as per the product manual. Media was spun at 3,000xg for 15 min intervals until 90-95% volume reduction. The retentate was then stored at -80*C.

Reelin Secretion and Dab1 Phosphorylation Confirmation via Western Blot: SDS-PAGE (sodium dodecyl sulfate polyacrylamide gel electrophoresis) and western blots were performed via the NuPAGE system: NuPAGE LDS (lithium dodecyl sulfate) Buffer (Invitrogen, NP0008), NuPAGE Sample Reducing Agent (10X) (Invitrogen, NP0004), NuPAGE Antioxidant (Invitrogen, NP0005), NuPAGE Transfer Buffer (20X) (Invitrogen, NP00061). For Reelin, 3-8% Tris-Acetate Protein gels were used (Invitrogen, EA03752BOX) with NuPAGE Tris-

Acetate SDS Running Buffer (Invitrogen, LA0041) and the HiMark Pre-Stained Protein Standard (Invitrogen, LC5699). 15 uL of conditioned media and 50 ug of concentrated protein in LDS were put in each well of SDS PAGE gel, which was blotted onto a PVDF membrane. Blocking was performed with 5% milk in TBS-T (0.2% tween 20) for one hr at RT. Antibodies used were: 1:1,000 Mouse Anti-Reelin antibody [G10] in 5% milk for two hr at RT and 1:10,000 Goat Anti-Mouse IgG H&L HRP-conjugated antibody in 5% milk for one hr at RT. For Dab1, 4-12% Bis-Tris Protein gels were used (Invitrogen, NP0322BOX) with NuPAGE MOPS (3-(N-morpholino)propanesulfonic acid) SDS Running Buffer (Invitrogen, NP0001) and the Novex Sharp Pre-Stained Protein Standard (Invitrogen, LC5800). Cells were lysed with radio-immunoprecipitation assay (RIPA) lysis buffer containing: 150 mM NaCl (Fisher Scientific, 7647-14-5), 1% NP-40 (Thermo Scientific, 85124), 0.5% sodium deoxycholate (Thermo Scientfic, 89904), 0.1% SDS (MP Biomedicals, 190522), 50 mM Tris-hydrochloride (Fisher Scientific, BP153-1), pH 8.0 with fresh protease (Thermo Scientific, 88666) and phosphase inhibitors (Thermo Scientific, 88667). Homogenates were centrifuged for 15 mins at 14,000 rcf in 4°C. Protein concentration of supernatant was found with BCA (bicinchoninic acid) with BSA (bovine serum albumin) (Thermo Scientific, 23227). 50 ug of protein in LDS was loaded into each well. SDS PAGE gel ran for one hr at 200 V, then blotted onto PVDF (polyvinyldiene difluoride) membranes for 75 mins at 30V on a cold plate to prevent overheating. Blocking was done with 5% BSA in TBS-T (0.2% tween 20) one hr RT. Antibodies are as listed: 1:10,000 Rabbit Anti-Dab1 (phospho Y232) antibody [EPR2247(2)] (abcam, ab126728), 1:15,000 Rabbit Anti-GAPDH (glyceraldehyde 3-phosphate dehydrogenase) antibody [EPR16891](abcam, ab181602), 1:2,000 Rabbit Anti-Dab1 (C-terminal) (Sigma, D1569), and 1:10,000 Goat Anti-Rabbit IgG H&L HRP-conjugated antibody (abcam, ab97051) in 5% BSA. Primary antibodies were incubated O/N at

4°C, while the secondary antibodies were incubated one hr at RT. All blots imaged with ECL substrate on a Kodak Image Station 4000mm PRO imager. Blots were then quantified by densitometry using ImageJ.

2.4 Migration Assays.

Wound Healing Assay with Doses of Concentrated Reelin Protein on Laminin: Each well of a 96-well tissue-culture treated plate (Thermo Scientific, 1520380) was treated with 5 ug/cm^2 laminin (Corning, 354232). Wells were scratched with a scalpel on the bottom for reference during imaging. SZ iHNSCs were accutased into single cell suspension and plated in NT2 medium. Serum differentiation was allowed to continue for 16 days, until a flat, uniform layer of with bipolar cells became evident. Cells were incubated in DMEM only for 24 hr prior to treatment. One scratch was made per well using a 200 uL micropipette tip and gently washed once with NT2 medium. Wells were treated with the following conditions: whole pCRL-transfected HEK cell-conditioned media, whole pCDNA-transfected HEK cell-conditioned media, 1:10 concentrated Reelin in fresh NT2, 1:10 concentrated control in fresh NT2, 1:30 concentrated Reelin in fresh NT2, 1:30 concentrated control in fresh NT2, 1:100 concentrated Reelin in fresh NT2, 1:100 concentrated control in fresh NT2, 1:300 concentrated Reelin in fresh NT2, 1:300 concentrated control in fresh NT2, 1:1,000 concentrated Reelin in fresh NT2, 1:1,000 concentrated control in fresh NT2. Wells were imaged at 4x before and after 14 hr incubation with a Leica DM IL microscope. Area of wounds found using MRI Wound Healing Tool on ImageJ.

Neuronal Migration Confirmation via ICC of Scratch Assay: Each well of the 96-well plate from the migration experiment was pre-fixed with cold 4% paraformaldehyde (PFA) (50% final concentration of media), and then fixed with total 4% PFA on ice. Blocking was performed with

5% BSA in Phospate-Buffered Saline with 0.1% Tween (PBS-T) and 7.51 g/mL glycine (Fisher, BP381-500). Rabbit-host anti-Beta-III-Tubulin (BIIIT) antibodies (abcam, ab18207) at 1:2000 and mouse-host anti-Glial Fibrillary Associated Protein (GFAP) antibodies (abcam, ab190288) at 1:1000 were co-incubated O/N at 4°C. Fluorescein Isothiocyanate (FITC)-conjugated donkey-host anti-mouse antibodies (Jackson, 715-095-150) and Tetramethylrhodamine (TRITC)-conjugated donkey host anti-rabbit antibodies (Jackson, 711-025-152) at 1:100 were incubated one hr at room temperature (RT) in a humidified chamber. DAPI (4',6-diamidino-2-phenylindole, dihydrochloride) (Invitrogen, D3571) was applied as per product manual and the cells were imaged with a Zeiss AX10 fluorescent microscope.

Chemotaxic and Invasion Assay with Whole Transfected HEK-Cell Conditioned Media: Chemotaxic and invasion assays were performed on 10-day old SZ iNPCs in a 24-well insert with a 12 um membrane (Millipore, PIXP01250). The chemotaxic assay was performed with 12 uncoated well inserts, while 12 were coated with 5 ug/cm^2 laminin (as per product sheet) to provide the extracellular matrix for the invasion assay. Cells were serum starved for 24 hr prior to treatment. Cells were treated with either the control whole cell-conditioned media from pCDNA-transfected HEK cells or whole pCRL-transfected HEK cell-conditioned media for 24 hr in 37*C, 5% CO2. Then the top/inside of the cell inserts were wiped thoroughly with an autoclaved cotton swab and gently washed with NT2 to ensure no cells were left within the insert. Culture medium was replaced with NT2 and 10% alamarBlue. Samples were transferred to a 96-well plate at time zero and at 24 hr, as well as a 0% reduction (fresh NT2 + 10% alamarBlue) and a 100% reduction control (autoclaved fresh NT2 + 10% alamarBlue). The absorbance was read at 630 nm and 540 nm via microplate reader, and the % reduction calculated using the formulas given in the alamarBlue product manual.

Invasion Assay with Doses of Concentrated Reelin Protein:

Chemotaxic and invasion assays were performed on 19-day old SZ iNPCs in a 24-well insert with a 12 um membrane (Millipore, PIXP01250) coated with 5ug/cm^2 laminin, as per product sheet. Cells were serum starved for 24 hr prior to treatment. . To ensure no cells had migrated through during iHNSC differentiation, well insert bottoms were wiped gently with an autoclaved cotton swab and then transferred to a fresh 24-well plate. Wells were treated for 24 hr in 37*C, 5% CO2 with the following conditions: whole pCDNA-transfected HEK cell-conditioned media, whole pCRL-transfected HEK cell-conditioned media, 1:10 concentrated Reelin in fresh NT2, 1:100 concentrated Reelin in fresh NT2, 1:1000 concentrated Reelin in fresh NT2, 1:10,000 concentrated Reelin in fresh NT2. Then the top/inside of the cell inserts were wiped thoroughly with an autoclaved cotton swab and gently washed with NT2 to ensure no cells were left within the insert. Culture medium was replaced with NT2 and 10% alamarBlue. Samples were transferred to a 96-well plate at time zero and at 48 hr, as well as a 0% reduction (fresh NT2 + 10% alamarBlue) and a 100% reduction control (autoclaved fresh NT2 + 10% alamarBlue). The absorbance was read at 630 nm and 540 nm via microplate reader, and the % reduction calculated using the formulas given in the alamarBlue product manual.

alamarBlue Proliferation Assay: SZ iHNSCs were accutased into single cell suspension and plated in NT2 medium at 2 x 10^4 cells/mL into a sterile 96-well tissue culture-treated plate (Costar, 3599). Cells were incubated at 37*C, 5% CO2 until adherence. NT2 media was replaced with pCRL/pEGFP-cotransfected or pcDNA/pEGFP-cotransfected HEK cell-conditioned media and 10% alamarBlue. Absorbance was measured by microplate reader at time zero, one, two three, five, six, seven, and 24 hr. 100% reduced alamarBlue was made via autoclave.

III. RESULTS

3.1 Neural induction and serum differentiation of iPS cells.

iPS cell colonies derived from a SZ fibroblast sample via Oct4, Sox2, Klf4, and c-Myc transfection were acquired and grown on MEFs. During neural induction, the iPS cell colonies in 20% FBS underwent morphological changes. Small, round, flattened colonies began to stick together becoming large and globular (**Figure 3**). Once removed from the neural induction medium, the cells were cultured in HNSC medium and passaged to keep the colonies small and proliferating. During the first few passages, floating colonies were separated from larger, partially differentiated, adherent unipolar and bipolar single cells. The adherent cells appear morphologically similar to neuroblasts, thereby indicating the potential for differentiation into neural subtypes. PCR on this sample confirms the presence of CD133 and BIIIT (**Figure 4)**, demonstrating that both HNSCs and neuronal cells are present in the culture.

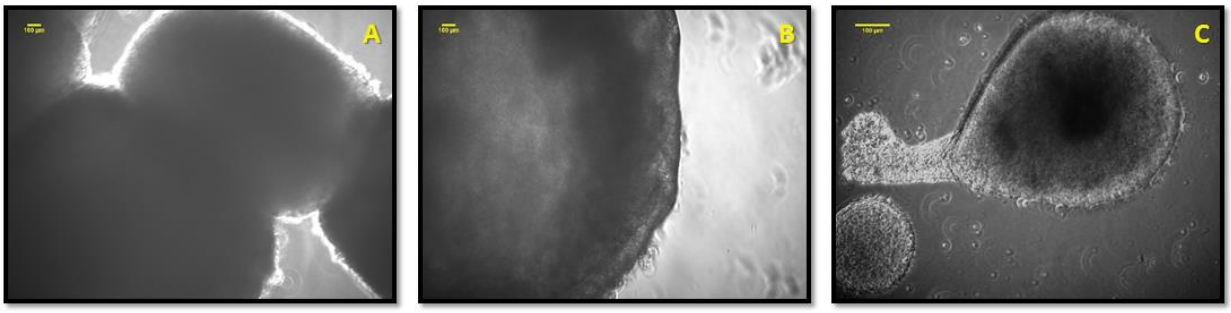

Figure 3: Time course images of neural induction. A. iPS cell colonies in neural induction medium for 2 days, 4x. B. Colony after 5 days in neural induction medium, 4x. C. Cell colonies cultured and passaged in the manner of HNSCs for 20 days after neural induction. Images representative of colonies in the culture vessel, 10x.

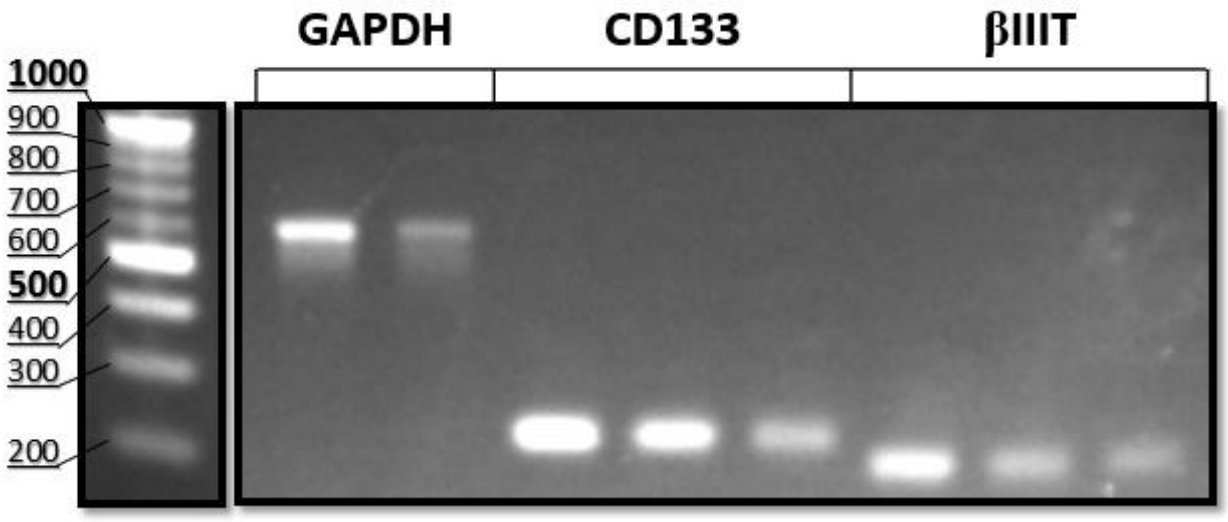

Figure 4: rt-PCR product in DNA gel electrophoresis of differentiated iPS cells after neural induction. Replicates came from the same iPS cell-derived HNSC culture. Neural induction was extraordinarily effective, as some cells overshot the CD133-expressing HNSC stage to differentiate into beta-III-tubulin (BIIIT)-expressing neurons.

The floating iHNSC colonies were cultured separately to prevent further differentiation. After two passages, the iHNSCs were placed in media with 10% FBS to establish their ability to differentiate. **Figure 5** represents the morphological changes that occur over time during serum differentiation of HNSCs. We can see small, spherical cells change into unipolar cells, then into larger bipolar cells; and then finally, terminally differentiating in to a cell with long, numerous processes. An ICC at day 10 of serum differentiation demonstrates bipolar immature neurons stained with BIIIT in equal measure with broad astrocytes stained with GFAP (**Figure 6**). A number of cells remained unstained except by DAPI, suggesting these cells were not yet differentiated.

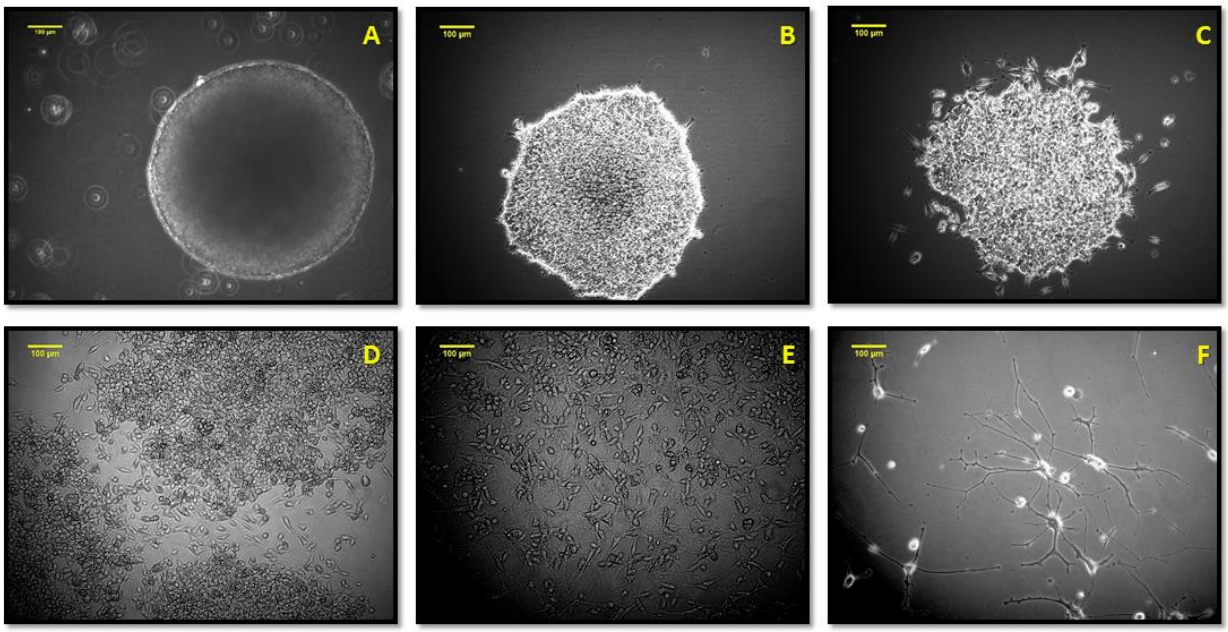

Figure 5: Time course images of SZ iHNSCs during serum differentiation. Images representative of whole cell culture, 10x. Scale bar: 100µm. A. Day 0. B. Day 1. C. Day 2. D. Day 3. E. Day 7. F. Day 20.

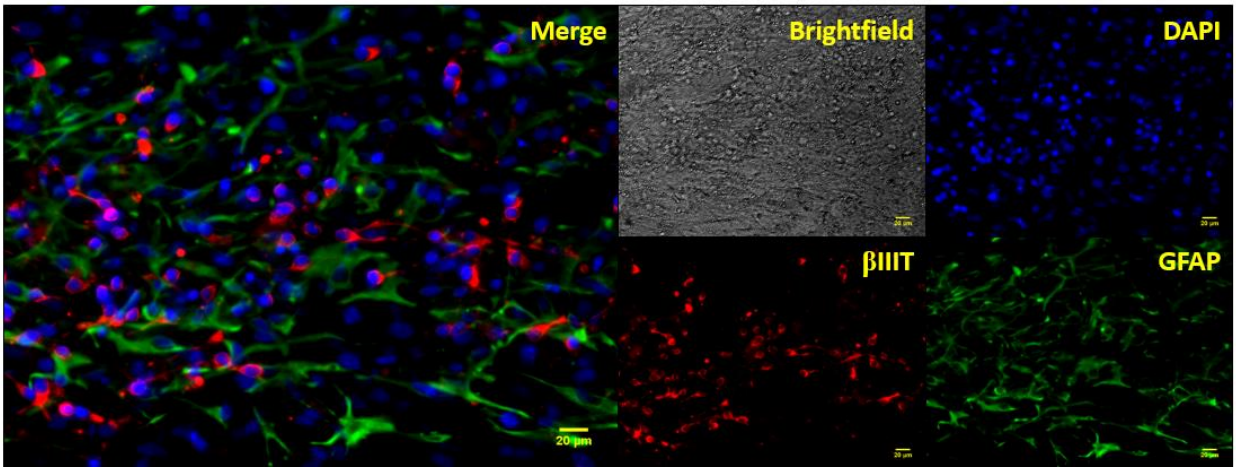

Figure 6: ICC of serum differentiated SZ iHNSCs at Day 10. Images representative of whole cell culture. Neurons stained for beta-III-tubulin (red). Glia stained for glial fibrillary acidic protein (green), 10x. Scale Bar: 20 µm.

3.2 Confirmation of pCRL plasmid and HEK293 Co-transfection with pEGFP.

The pCRL plasmid was created 22 years ago by G. D'Archangelo and T. Curran[6], who gifted it to the lab. To validate the continuing presence of the *RELN* gene and to detect any potential degradation, rt-PCR was performed on amplified and isolated pCRL plasmid from four different clones and the product ran in a DNA electrophoresis gel (**Figure 7**). All four clones demonstrate a band at the expected size of 101 base pairs (bp), indicating the presence of the *RELN* gene. The Fast Digest enzyme digest products for the pCRL plasmid at the BamHI and EcoRI cutsites were also run through the same gel. The BamHI enzyme digest products resulted in two bands at approximately the expected sizes of 10.6 and 5.4 kilobase pairs (kb), indicating a full digest of the plasmid. However, the EcoRI enzyme digest demonstrates an incomplete digestion with a strong band at ~10.6 and no band at the expected 400 bp; however, two bands appear approximately at the expected size of 5.8/5.4 and 4.4 indicating an incomplete digestion. The expected 5.8 and 5.4 bands are assumed to be too close together to be resolved. However, there are no fragments at unexpected band sizes. This combined with the success of the PCR, BamHI enzyme digest, and the lack of fragments when whole plasmid is loaded in the gel, we can conclude that the pCRL gene was intact.

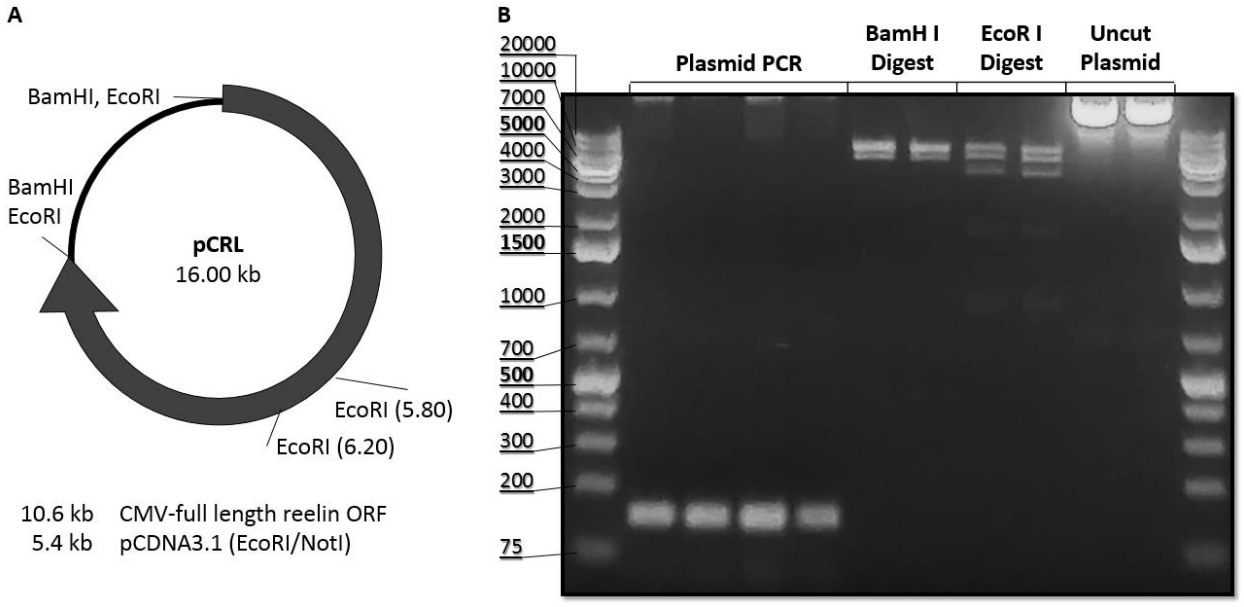

Figure 7: RELN pCRL plasmid. A. Abbreviated map of pCRL plasmid. Illustration includes only the EcoRI and BamHI cut sites used. B. Gel Electrophoresis of plasmid PCR product, restriction enzyme digest products, and uncut plasmid

HEK293 cells were transfected with either pCRL + pEGFP or pCDNA3.1 + pEGFP and monitored for eGFP expression for two days. After this point, the media was changed to standard HEK293 cell culture media (**Figure 8**). To ensure the secretion of the pCRL protein product, media was collected from each sample and a dot blot was performed (**Figure 9A**). The dot blot presented with a small amount of background in the wells with pCDNA-transfected HEK293 cell-conditioned medium, perhaps due to the high amount of protein in FBS. However, the pCRL-transfected HEK293 cell-conditioned medium appears to have a stronger reaction indicating Reelin presence in this medium. To be certain, a western blot was performed on whole medium, concentrated Reelin retentate, and the left over filtrate for two different collection times for both the pCRL- and pCDNA-transfected HEK cell cultures (**Figure 9B**). The first collection of medium seems to contain less Reelin than the second, from the cell cultures that were

transfected with pCRL. This may be due to the first undergoing a freeze-thaw cycle, while the second was fresh, or due to the cells secreting less Reelin protein in the initial days after transfection. To ensure even distribution of Reelin protein product, the collections thereafter were pooled for concentration and treatment. Nevertheless, Reelin protein can be seen at its three expected band sizes (~388, ~280, ~160 kDa) faintly in the media and more strongly in the retentates. As expected, there is no Reelin in the filtrates or in the pCDNA-transfected HEK293 cell-conditioned media retentates. The three band sizes are from the desired full-length Reelin protein and its two cleaved isoforms.

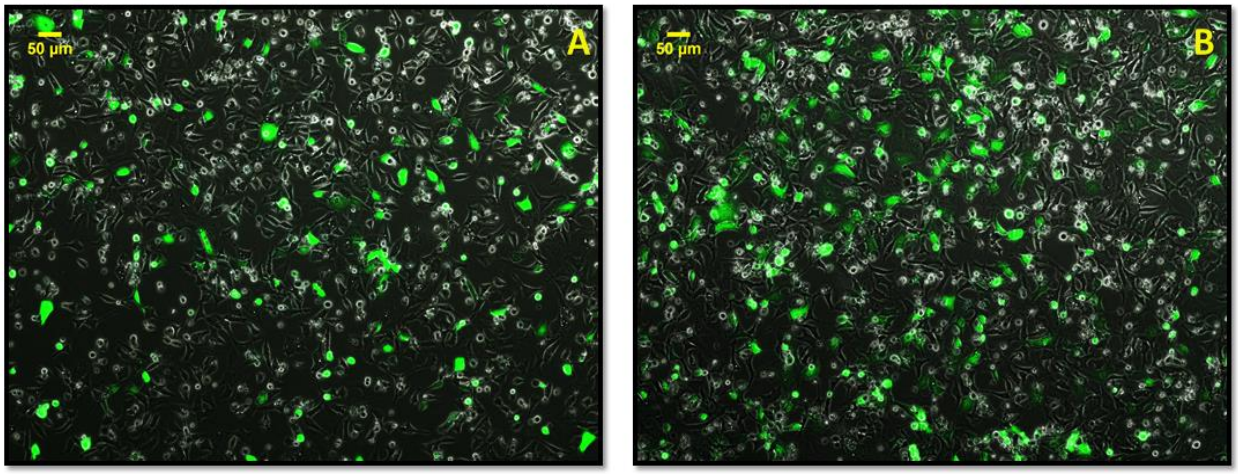

Figure 8: pCRL and pEGFP co-transfected HEK 293 cells. Representative merged GFP and brightfield images. A. 17 hr transfection, 10x. B. 41 hr transfection, 10x.

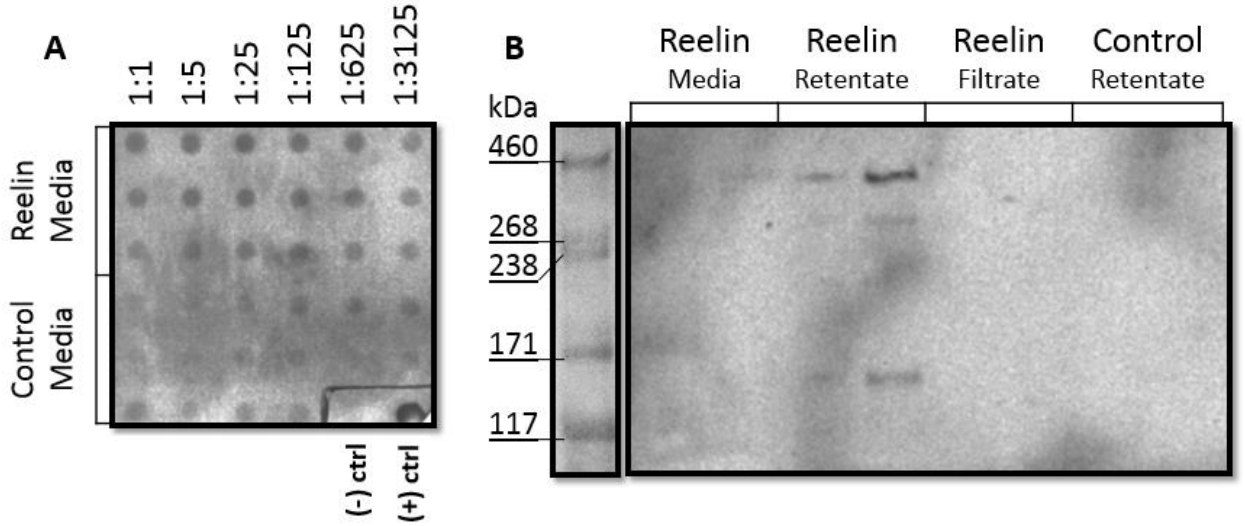

Figure 9: Transfected-HEK293 cell Reelin protein expression. A. Dot Blot of pCRL (Reelin) or pCDNA (Control) and pEGFP co-transfected-HEK293 cell-conditioned whole media in dilution. (-) ctrl: technical negative control consisting of deionized water. (+) ctrl: technical positive control consisting of pure anti-Reelin antibody. B. Western blot of two collections of transfected HEK293 cell-conditioned whole Reelin media (Lanes 1 and 2), concentrated retentate of Reelin media (Lanes 3 and 4), filtrate for Reelin media (Lanes 5 and 6), and concentrated retentate of Control media (Lanes 7 and 8). Lanes 3 and 5 are from concentrating medium from the sample in Lane 1. Lanes 4 and 6 are from concentrating medium from Lane 2. Lane 7 was collected and concentrated at the same time as Lane 3. Lane 8 was collected and concentrated at the same time as Lane 4.

3.3 iPS cell-derived NPCs' molecularly respond to Reelin.

The first cytosolic protein modified in the Reelin signaling pathway is Dab1, which is activated via phosphorylation of 5 different tyrosine residues, including Y232.[72] To ensure the Reelin treatment has an effect within the cell, phosphorylated Dab1 was measured via SDS-PAGE and western blotting. If we look only at phosphorylation (**Figure 10**), there is the same relative amount in the SZ iNPC samples treated with concentrated Reelin transfected-HEK293 cell-conditioned medium as those treated with concentrated pCDNA transfected-HEK293 cell-condition medium (ANOVA, $p = 0.16916$, $F_{observed}(2.80698) < F_{critical}(7.70864)$). As it has been established, Reelin targets Dab1 for degradation via polyubiquination as a negative feedback loop reducing the total

amount of Dab1.[8] Although their differences were not significant in an LSD post-hoc test, can see this general effect in the total Dab1 of the SZ cells treated with Reelin versus the control cells (ANOVA, $p = 0.09046$, $F_{observed}(4.93499) < F_{critical}(7.708647)$). Once the relative total Dab1 protein concentration is factored in, we see that there is more phosphorylated Dab1 per total amount of Dab1 protein present in Reelin-treated SZ iNPCs ($M = 3.53992$, $SE = 0.67720$) than the Control-treated SZ iNPCs ($M = 1.12071$, $SE = 0.21995$) (LSD, $p = 0.05$, $t_{observed}(2.41921) > t_{critical,\ two\text{-}tail}(1.39788)$)

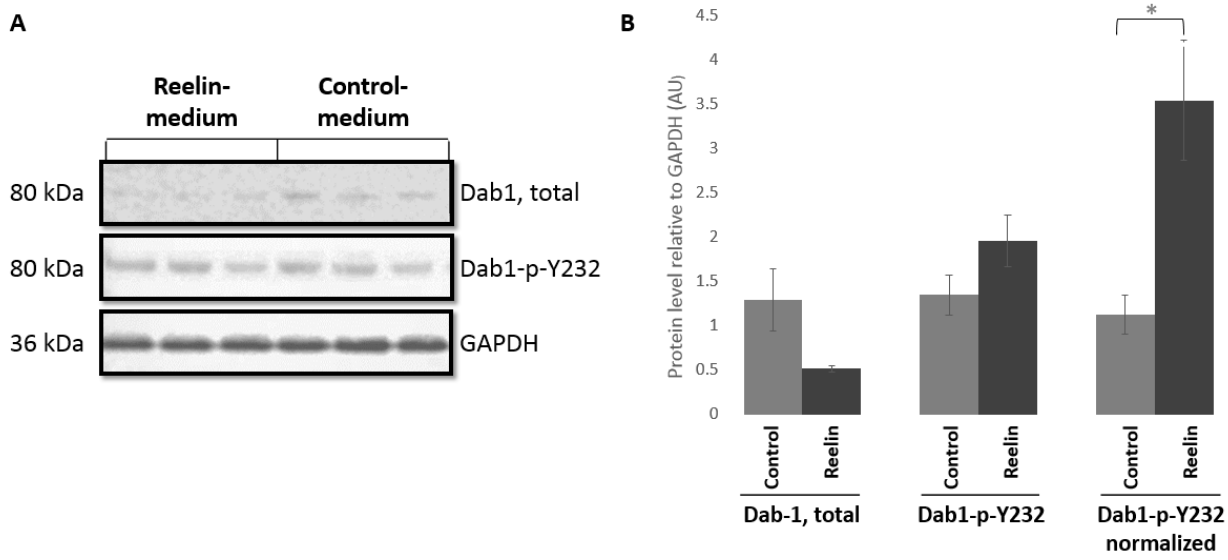

Figure 10: Dab1 Phosphorylation. A. Western blot of SZ iNPCs treated with pCRL-transfected HEK293 cell-condition medium (Reelin-medium) versus pCDNA-transfected HEK293 cell-condition medium (Control-medium). B. Bar graph of adjusted relative densities of total Dab1, Dab1-p-Y232, and Dab1-p-Y232 normalized to the total amount of Dab1. *p = 0.05

3.4 SZ iPS cell-derived NPCs have increased wound closure when treated with Reelin.

The most common and well-established assay performed when studying migration is the scratch assay. It's simple but elegant design allows for straightforward, accessible imaging and ICC. To

investigate whether SZ iNPCs respond to Reelin, we plated iHNSCs at high confluence and allowed them to differentiate until the formation a, relatively, uniform carpet of cells consisting of mainly bipolar morphology. We, then, serum starved the cells for 24 hr before the scratch occurred to prevent confounding data due to proliferation. Since the treatment is an unusually large protein expressed via transfected-HEK 293 cells, we partially purified it via protein concentration with a membrane that retains proteins over 100kDa. A dose assay was then performed to find the optimal relative concentration of Reelin for migration. In all the dilution sets – except 1:1000 – the Control-treated SZ iNPCs migrated significantly less than the Reelin-treated SZ iNPCs (**Figure 11**) (LSD, p = 0.05: Reelin-medium v. Control-medium, $t_{observed,\ two\text{-}tail}(9.09820) > t_{critical,\ two\text{-}tail}(3.75058)$; Reelin v. Control 1:10, $t_{observed}(6.55384) > t_{critical,\ two\text{-}tail}(3.72147)$; Reelin v. Control 1:30, $t_{observed}(8.46283) > t_{critical,\ two\text{-}tail}(3.79604)$; Reelin v. Control 1:100, $t_{observed}(12.9099) > t_{critical,\ two\text{-}tail}(3.84566)$; Reelin v. Control 1:300 $t_{observed}(9.49628) > t_{critical,\ two\text{-}tail}(4.10019)$; Reelin v. Control 1:1000, not significant (ns), $t_{observed}(3.02300) < t_{critical,\ two\text{-}tail}(3.84566)$). The highest percent wound closure is seen when the concentrated Reelin-medium was diluted 1:100 (M = 70.3951, SE = 1.16939), which is significantly higher than all the other doses (LSD, p = 0.05: Reelin-medium v. 1:100 $t_{observed}(4.02585) > t_{critical,\ two\text{-}tail}(2.05387)$; Reelin 1:10 v. 1:100, $t_{observed}(4.85176) > t_{critical,\ two\text{-}tail}(2.06052)$; Reelin 1:30 v. 1:100, $t_{observed}(3.73506) > t_{critical,\ two\text{-}tail}(2.05156)$; Reelin 1:100 v. 1:300, $t_{observed}(2.09460) > t_{critical,\ two\text{-}tail}(2.03887)$; Reelin 1:100 v. 1:1000, $t_{observed}(7.57249) > t_{critical,\ two\text{-}tail}(2.08350)$). The controls are overall similar, regardless of dilution (ANOVA, p = 0.934453, $F_{observed}(0.258898) > F_{critical}(2.299234)$).

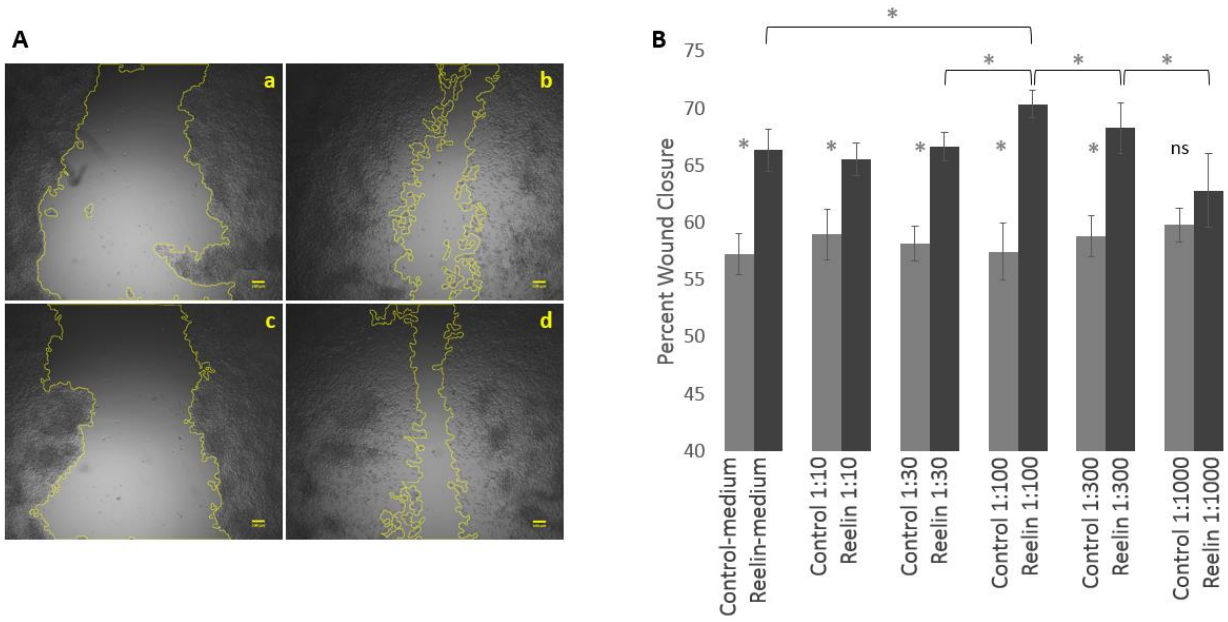

Figure 11: **Scratch Assay of Reelin-treated SZ iNPCs.** A. Representative images of SZ iNPCs, treated with 1:100 dilutions of concentrated pCRL-transfected HEK cell-conditioned medium (Reelin 1:100) or pCDNA-transfected HEK cell-conditioned medium (Control 1:100), 4x. Scale Bar: 100 μm. a. t(0hr), SZ iNPCs in Control 1:100. b. t(14hr), SZ iNPCs in Control 1:100. c. t(0hr), SZ iNPCs in Reelin 1:100. d. t(14hr), SZ iNPCs in Reelin 1:100. B. Bar graph of percent wound closure of SZ iNPCs, treated with whole or dilutions (1:10, 1:30, 1:100, 1:300, 1:1000) of concentrated pCRL-transfected HEK cell-conditioned media (Reelin) or pCDNA-transfected HEK cell-conditioned media (Control). *p = 0.05, ns – not significant

To verify that neurons were indeed migrating, we performed ICC on the scratch immediately after the second set of photos was taken (t = 14 hr). Bipolar βIIIT-positive immature neurons are seen within the healed scratch, as well as some GFAP-positive glia (**Figure 12**). Some cells express both proteins, indicating they are neural cells that are not yet committed to a specific fate.

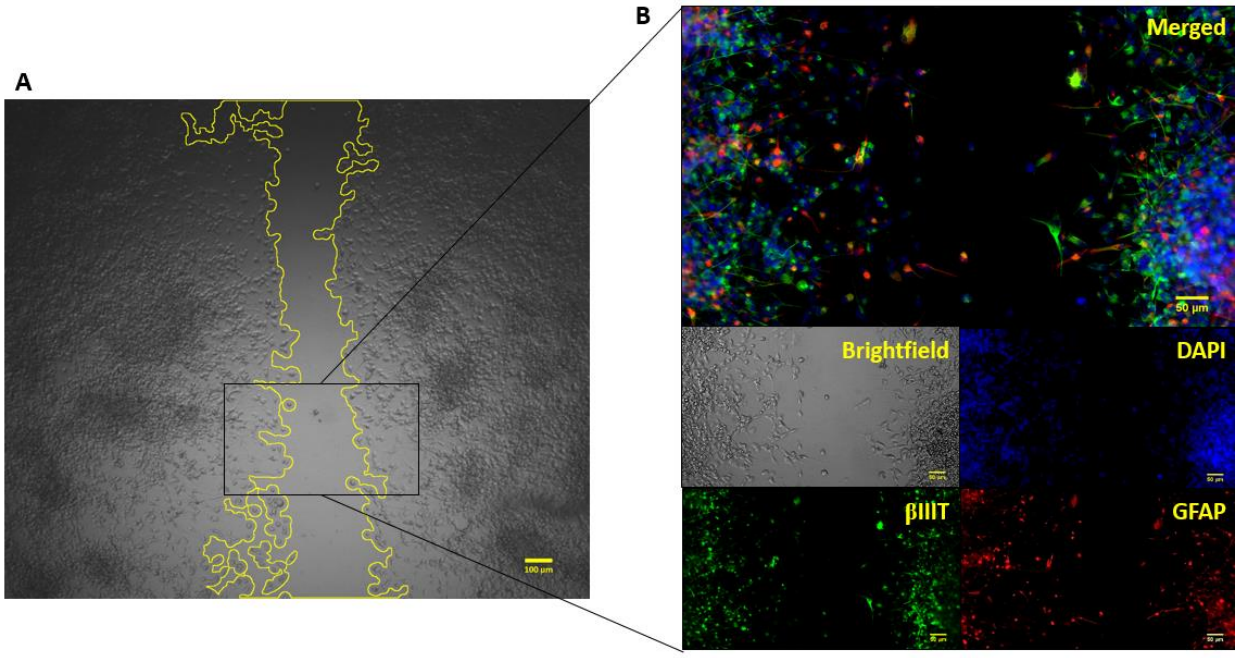

Figure 12: **ICC of neurons in scratch assay.** A. Representative image of scratch at t(14hr), SZ iNPCs in Reelin 1:100, 4x. Scale Bar: 100 µm. B. ICC of SZ iPS-cell derived neurons migrating into the wound in the presence of Reelin. Neurons stained with beta-III-tubulin (green). Glia stained with glial fibrillary acidic protein (red), 10x. Scale Bar: 50 µm.

3.5 SZ iPS cell-derived NPCs demonstrate increased invasion when treated with Reelin.

During corticogenesis, neurons travel through the previous laminae of the cortex to form the next layer into the Reelin gradient. While scratch assay are useful for visualization, chemotaxic and invasion assays more accurately replicate the 3-dimensional, *in vivo* processes by which cells migrate. To that end, SZ iNPCs were cultured inside a cell insert that was either coated with laminin or not, then treated with Reelin-medium or Control-medium. Using the alamarBlue assay for proliferation, we were able quantitatively measure how much migration occurred to the other side of the insert. In **Figure 13A** you can see that with or without laminin coating, the Reelin-treated SZ iNPCs migrated through the membrane significantly more than the Control-treated SZ iNPCs. (LSD, $p = 0.05$: Reelin-medium v. Control-medium without laminin, $t_{observed,\ two-}$

$_{tail}(3.75058) > t_{critical, two\text{-}tail}(9.09820)$; Reelin-medium v. Control with laminin, , $t_{observed, two\text{-}tail}(22.43208) > t_{critical, two\text{-}tail}(9.09820)$. Interestingly, while both Control-treated conditions resulted in similar outcomes (LSD, ns, Control-medium without laminin v. with laminin, $t_{observed, two\text{-}tail}(6.014094) < t_{critical, two\text{-}tail}(9.09820)$, the Reelin-treated iNPCs treated with laminin migrated significantly more than the Reelin-treated iNPCs without laminin (LSD, p = 0.05: Reelin-medium without laminin v. with laminin, $t_{observed, two\text{-}tail}(18.12433) > t_{critical, two\text{-}tail}(9.09820)$, suggesting a synergistic effect between the two proteins. In the dose assay, we can see a pattern similar to the doses during wound closure (**Figure 13B**). The most migration occurred at the 1:100 Reelin dose treatment (M = 42.9120, SE = 2.16437), which was significantly higher than all the other conditions (LSD, p = 0.05; Reelin whole medium v. 1:100, $t_{observed, two\text{-}tail}(5.94737) > t_{critical, two\text{-}tail}(4.87795)$; Reelin 1:10 v. 1:100, $t_{observed, two\text{-}tail}(17.7839) > t_{critical, two\text{-}tail}(4.87795)$; Reelin 1:100 v. 1:1,000, $t_{observed, two\text{-}tail}(9.99575) > t_{critical, two\text{-}tail}(4.51611)$; Reelin 1:100 v. 10,000, $t_{observed, two\text{-}tail}(6.12553) > t_{critical, two\text{-}tail}(4.51611)$. The Reelin whole medium (M = 36.9646, SE = 2.38307) the Reelin 1:1,000 (M = 32.9162, SE = 1.04009), and Reelin 1:10,000 medium (M = 36.7864, SE = 1.32409) conditions were all similar and their differences not significant. The most unusual condition would be the Reelin 1:10, which demonstrates the least amount of migration (M = 25.1281, SE = 0.3968086) perhaps due to the concentration of Reelin inducing maturation and spine formation rather than migration. More research is required to discover the point at which this chemical message switches from one to the other.

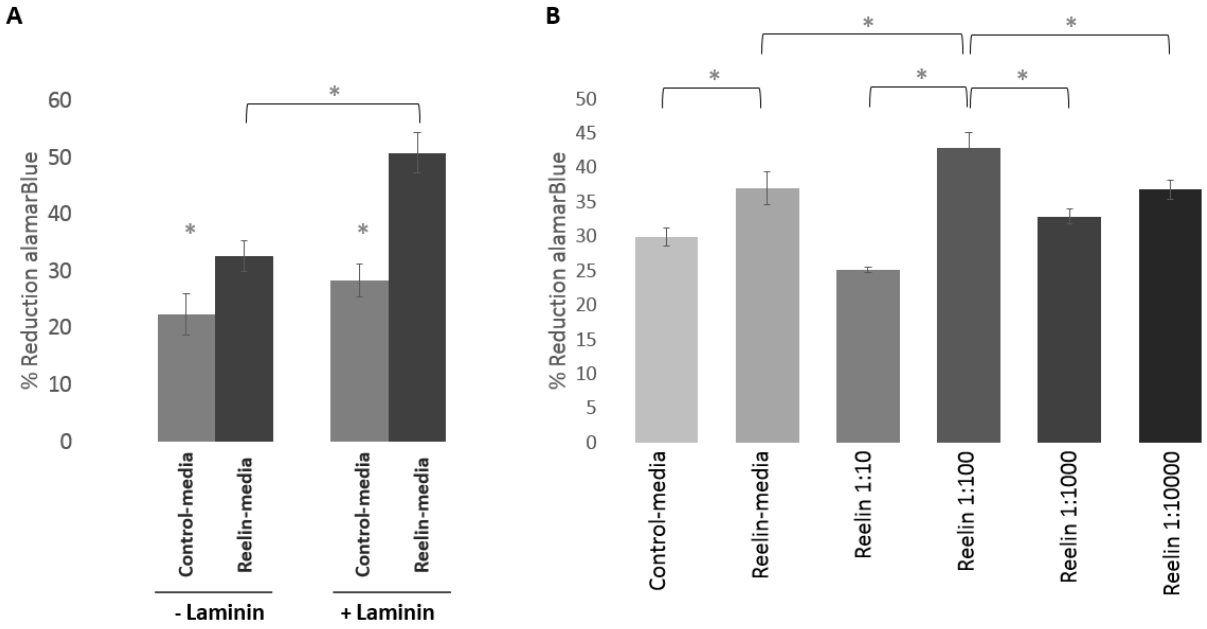

Figure 13: **Invasion Assay.** A. Bar graph of adjusted average change in absorbance of alamarBlue due to oxidation from SZ iNPCs, treated versus untreated +/- laminin. B. Bar graph of adjusted average change in absorbance of alamarBlue due to oxidation from SZ iNPCs, treated dilutions of concentrated pCRL- or pCDNA-transfected HEK cell-conditioned media

3.6 SZ iPS cell-derived NPCs do not show increased proliferation when treated with Reelin.

To ensure our results were due to migration and not confounded by the upregulation of proliferation, an alamarBlue proliferation assay was performed. When cells proliferate, the acidic byproducts result in increased reduction of the alamarBlue causing a color shift that can be measure by absorbance. The more alamarBlue that is reduced, the lower the absorbance. We can see in **Figure 14** that SZ iNPCs treated with Reelin-medium grow at the same rate as those treated with Control-medium (LSD, $p = 0.05$; time = 1 hr, $t_{observed,\ two\text{-}tail}(0.003667) < t_{critical,\ two\text{-}tail}(0.014671)$; time = 2 hr, $t_{observed,\ two\text{-}tail}(0.009267) < t_{critical,\ two\text{-}tail}(0.022248)$; time = 3 hr, $t_{observed,\ two\text{-}tail}(0.041067) < t_{critical,\ two\text{-}tail}(0.053876)$; time = 5 hr, $t_{observed,\ two\text{-}tail}(0.0392) < t_{critical,\ two\text{-}tail}(0.057230)$; time = 6 hr, $t_{observed,\ two\text{-}tail}(0.039467) < t_{critical,\ two\text{-}tail}(0.057208)$; time = 7 hr, $t_{observed,}$

$t_{two\text{-}tail}(0.034533) < t_{critical,\ two\text{-}tail}(0.059281)$; time = 24 hr, $t_{observed,\ two\text{-}tail}(0.003467) < t_{critical,\ two\text{-}tail}(0.073788)$)

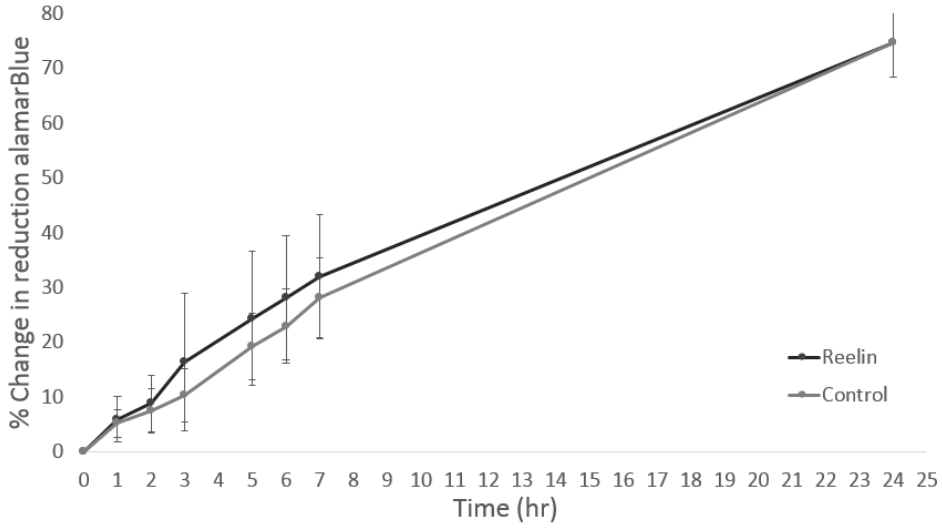

Figure 14: Proliferation with Reelin Treatment. Line graph of adjusted average change in absorbance of alamarBlue over time, treated versus untreated SZ iNPCs.

IV. CONCLUSION

In order to study the role of Reelin in SZ, we used a Reelin-deficient iPS cell line derived from a live SZ patient skin biopsy differentiated into NPCs. Initially, we established that the cell can molecularly receive the external Reelin signal and activate the pathway via Dab1 phosphorylation (**Figure 9**). Since, these SZ iNPCs previously exhibited migration dysfunction as compared to wild type cells under control conditions *in vitro* [57], we treated with exogenous Reelin and measured changes in the SZ iNPCs' cellular motility. These cells displayed increased wound closure (**Figure 11**), increased chemotaxis across a membrane and increased invasion through an ECM-coated membrane (**Figure 13A)**. We noted that while glia are known for migrating, neurons were also within the wound closure when treated with Reelin (**Figure 12**). In addition, we saw there was an optimal concentration of Reelin for migration **(Figure 11, Figure 13B)**. Lastly, Reelin-induced effects were shown to be due to migration and not proliferation **(Figure 14)**. Using the metric of cellular migration, we can see from this study that SZ iNPCs are indeed capable of receiving and reacting to extracellular Reelin treatment.

Since SZ causes are polyfactoral presenting with a myriad of signs and symptoms, the field has had a difficult time establishing models for mechanistic study. While the heterozygous *Reeler* mouse is the established model for the field, it may not mechanistically recapitulate the complex interplay involved with the Reelin pathway in SZ. Unknown parallel pathways in migration, dendrite formation, or synapse function may prevent Reelin treatment in a way that is not predictable by a mouse model. Post-mortem brains can tell us SZ patients have lower amounts of Reelin protein in their cortex and DNA mutations that contribute to a disease, but sample acquisition is limited to the end-point of the disease. Due to these restrictions and the complexity

of the disease, it was previously unknown whether or not SZ patient living cells would even respond to Reelin treatment or if Reelin treatment alone was sufficient to improve the disordered phenotype. Filling this niche in our body of knowledge, iPS cells are capable of being differentiated to any stage of development, while retaining the specific phenotypes and protein expressions that contributes to the disorder. Future experiments with SZ iPS cells can further discover the capabilities and limitation of Reelin pathway treatment for SZ with Reelin deficiency.

REFERENCES

1. S. Keilani, K. Sugaya, Reelin induces a radial glial phenotype in human neural progenitor cells by activation of Notch-I. *BMC Developmental Biology* **8**, (2008).
2. H. M. Kim *et al.*, Reelin function in neural stem cell biology. *PNAS* **99**, 4020-4025 (2002).
3. S. Niu, A. Renfro, C. Quattrocchi, M. Sheldon, G. D'Arcangelo, Reelin promotes hippocampal dendrite development through the VLDLR/ApoER2-Dab1 pathway. *Neuron* **41**, 71-84 (2004).
4. V. Borrell *et al.*, Reelin Regulates the Development and Synaptogenesis of the Layer-Specific Entorhino-Hippocampal Connections. **19**, 1345-1358 (1999).
5. G. D'Arcangelo *et al.* (J Neurosci. , 1997), vol. 17, pp. 23-31.
6. G. D'Arcangelo *et al.*, A protein related to extracellular matrix proteins deleted in the mouse mutant reeler. *Nature* **374**, 719-723 (1995).
7. C. Pesold, W. S. Liu, A. Guidotti, E. Costa, H. J. Caruncho. (Proc. Natl. Acad. Sci. USA, 1999), vol. 9, pp. 3217-3222.
8. T. Hiesberger *et al.*, Direct binding of reelin to VLDL receptor and ApoE receptor 2 induces tyrosine phosphorylation of disabled-1 and modulates tau phosphorylation. *Neuron* **24**, 481-489 (1999).
9. S. Qiu, E. J. Weeber, Reelin signaling facilitates maturation of CA1 glutamatergic synapses. *Journal of Neurophysiology* **97**, 2312-2321 (2007).
10. Y. Bamba *et al.*, Differentiation, polarization, and migration of human induced pluripotent stem cell-derived neural progenitor cells co-cultured with human glial

cell line with radial glial-like characteristics. *Biochemical and Biophysical Research Communications* **447**, 683-688 (2014).

11. R. Gorris *et al.*, Pluripotent stem cell-derived radial glia-like cells as stable intermediate for efficient generation of human oligodendrocytes. *Glia* **63**, 2152-2167 (2015).

12. M. Trommsdorff , J. P. Borg , B. Margolis , J. Herz, Interaction of cytosolic adaptor proteins with neuronal apolipoprotein E receptors and the amyloid precursor protein. *Journal of Biological Chemistry* **273**, 33556–33560 (1998).

13. Y. Jossin, J. A. Cooper, Reelin, Rap1 and N-cadherin orient the migration of multipolar neurons in the developing neocortex. *Nature Neuroscience* **14**, 697–703 (2011).

14. G. D'Arcangelo, Reelin in the Years: Controlling Neuronal Migration and Maturation in the Mammalian Brain. *Advances in Neuroscience* **2014**, (2014).

15. M. Frotscher, Dual role of Cajal-Retzius cells and reelin in cortical development. *Cell Tissue Research* **290**, 315–322 (1997).

16. J. A. Cooper, A mechanism for inside-out lamination in the neocortex. *Trends in Neuroscience* **31**, 113-119 (2007).

17. J. T. Rogers *et al.*, Reelin supplementation enhances cognitive ability, synaptic plasticity, and dendritic spine density. *Learning and Memory* **18**, 558-564 (2011).

18. M. Frotscher. (Springer-Verlag, Cell Tissue Research, 1997), vol. 290, pp. 315–322.

19. J. A. Cooper. (Cell Press, Trends in Neuroscience, 2007), vol. 31, pp. 113-119.

20. V. Borrell *et al.*, Reelin Regulates the Development and Synaptogenesis of the

Layer-Specific Entorhino-Hippocampal Connections. *The Journal of Neuroscience* **19**, 1345-1358 (1999).

21. D. R. Grayson *et al.*, The human reelin gene: transcription factors (+), repressors (-), and the methylation switch (+/-) in schizophrenia. *Pharmacology & Therapeutics* **111**, 272-286 (2006).

22. J. Herz, Y. Chen, Reelin, lipoprotein receptors, and synaptic plasticity. *Nature* **7**, 850-859 (2006).

23. M. Frotscher, Role for reelin in stabilizing cortical architecture. *Trends in Neurosciences* **33**, 407-414 (2010).

24. G. A. Yudowski, O. Olsen, H. Adensnik, K. W. Marek, D. S. Bredt, Acute inactivation of PSD-95 destabilizes AMPA receptors at hippocampal synapses. *PLoS ONE* **8**, e53965 (2013).

25. J. Iafrati, M. J. Orejarena, O. Lassalle, L. Bouamrane, P. Chavis, Reelin, an extracellular matrix protein linked to early onset psychiatric diseases, drives postnatal development of the prefrontal cortex via GluN2B-NMDARs and the mTOR pathway. *Molecular Psychiatry* **19**, 417-426 (2014).

26. M. Trommsdorff *et al.*, Reeler/Disabled-like Disruption of Neuronal Migration in Knockout Mice Lacking the VLDL Receptor and ApoE Receptor 2. *Cell* **97**, 689-701 (1999).

27. S. Niu, O. Yabut, G. D'Arcangelo, The Reelin Signaling Pathway Promotes Dendritic Spine Development in Hippocampal Neuron. *Journal of Neuroscience* **28**, 10339–10348. (2008).

28. S. E. Hong *et al.*, Autosomal recessive lissencephaly with cerebellar hypoplasia is associated with human RELN mutations. *Nature Genetics* **26**, 93-96 (2000).

29. I. Palacios-Garcia *et al.*, Prenatal stress down-regulates reelin expression by methylation of its promoter and induces adult behavioral impairment in rats *PLoS One* **10**, (2015).

30. L. Shi, S. H. Fatemi, R. W. Sidwell, P. H. Patterson, Maternal Influenza Infection Causes Marked Behavioral and Pharmacological Changes in the Offspring. *Journal of Neuroscience* **23**, 297–302 (2003).

31. U. Meyer, M. Nyffeler, B. K. Yee, I. Knuesel, J. Feldon, Adult brain and behavioral pathological markers of prenatal immune challenge during early/middle and late fetal development in mice. *Brain, Behavior, and Immunity* **22**, 469-486 (2008).

32. L. Harvey, P. Boksa, A stereological comparison of GAD67 and reelin expression in the hippocampal stratum oriens of offspring from two mouse models of maternal inflammation during pregnancy. *Neuropharmacology* **62**, 1767-1776 (2012).

33. W. S. Liu *et al.*, Down-regulation of dendritic spine and glutamic acid decarboxylase 67 expressions in the reelin haploinsufficient heterozygous reeler mouse. *PNAS* **98**, 3477-3482 (2001).

34. S. Qiu, L. F. Zhao, K. M. Korwek, E. J. Weeber, Differential Reelin-Induced Enhancement of NMDA and AMPA Receptor Activity in the Adult Hippocampus. *The Journal of Neuorscience* **26**, 12943-12955 (2006).

35. K. Sakai, H. Shoji, T. Kohno, T. Miyakawa, M. Hattoria, Mice that lack the C-terminal region of Reelin exhibit behavioral abnormalities related to neuropsychiatric disorders. *Scientific Reports* **6**, (2016).

36. E. J. Weeber *et al.*, Reelin and ApoE Receptors Cooperate to Enhance Hippocampal Synaptic Plasticity and Learning. *Journal of Biological Chemistry* **277**, 39944-39952 (2002).

37. H. Imai *et al.*, Dorsal Forebrain-Specific Deficiency of Reelin-Dab1 Signal Causes Behavioral Abnormalities Related to Psychiatric Disorders. *Cerebral Cortex* **27**, 3485-3501 (2017).

38. A. M. Barr, K. N. Fish, A. Markou, W. G. Honer, Heterozygous reeler mice exhibit alterations in sensorimotor gating but not presynaptic proteins. *The European Journal of Neuroscience* **27**, 2568-2574 (2008).

39. G. Laviola, E. Ognibene, E. Romano, W. Adriani, F. Keller, Gene-environment interaction during early development in the heterozygous reeler mouse: clues for modelling of major neurobehavioral syndromes. *Neuroscience and Biobehavioral Reviews* **33**, 560-572 (2009).

40. M. Tochigi *et al.*, Methylation status of the reelin promoter region in the brain of schizophrenic patients. *Biological Psychiatry* **63**, 530-533 (2008).

41. H. M. Abdolmaleky *et al.*, Hypermethylation of the reelin (R*ELN*) promoter in the brain of schizophrenic patients: A preliminary report. *Am. J. Med. Genet.* **134B**, 60-66 (2005).

42. W. Li, X. Guo, S. Xiao, Evaluating the relationship between reelin gene variants (rs7341475 and rs262355) and schizophrenia: A meta-analysis. *Neuroscience Letters* **16**, 42-47 (2015).

43. Y. Liu *et al.*, Replication of an association of a common variant in the Reelin gene (RELN) with schizophrenia in Ashkenazi Jewish women. *Psychiatric Genetics* **20**, 184-186 (2010).

44. S. Shifman *et al.*, Genome-wide association identifies a common variant in the reelin gene that increases the risk of schizophrenia only in women. *PLoS Genetics 2008* **4**, e28 (2008).

45. J. Ekelund *et al.*, Genome-wide scan for schizophrenia in the Finnish population: evidence for a locus on chromosome 7q22. *Human Molecular Genetics* **9**, 1049-1057 (2000).

46. H. Hall *et al.*, Potential genetic variants in schizophrenia: a Bayesian analysis. *World Journal of Biological Psychiatry* **8**, 12-22 (2007).

47. W. J. Kuang, R. F. Sun, Y. S. Zhu, S. B. Li, A new single-nucleotide mutation (rs362719) of the reelin (RELN) gene associated with schizophrenia in female Chinese Han. *Genetic Molecular Research* **10**, 1650-1658 (2011).

48. G. Ovadia, S. Shiftman, The Genetic Variation of R*ELN* Expression in Schizophrenia and Bipolar Disorder. **6**, (2011).

49. F. Impagnatiello *et al.*, A decrease of reelin expression as a putative vulnerability factor in schizophrenia. *PNAS* **95**, 15718-15723 (1998).

50. A. Guidotti *et al.*, Decrease in reelin and glutamaic acid decarboxylase$_{67}$ (GAD$_{67}$) expression in schizophrenia and bipolar disorder: a postmortem brain study. *Arch Gen Psychiatry* **57**, 1061-1069 (2000).

51. S. Eastwood, P. Harrison, Interstitial white matter neurons express less reelin and are abnormally distributed in schizophrenia: toward an integration of molecular and morphologic aspects of the neurodevelopmental hypothesis. *Molecular Psychiatry* **8**, 821-831 (2003).

52. S. H. Fatemi, J. A. Earle, T. McMenomy, Reduction in Reelin immunoreactivity in hippocampus of subjects with schizophrenia, bipolar disorder and major depression. *Molecular Psychiatry* **5**, 654-663 (2000).

53. D. Joshi, S. J. Fung, A. Rothwell, C. S. Weickert, Higher gamma-aminobutyric acid neuron density in the white matter of orbital frontal cortex in schizophrenia. *Biological Psychiatry* **72**, 725-733 (2012).

54. P. Falkai, T. Schneider-Axmann, W. G. Honer, Entorhinal cortex pre-alpha cell clusters in schizophrenia: quantitative evidence of a development abnormality. *Biological Psychiatry* **47**, 937-943 (2000).

55. L. A. Glantz, D. A. Lewis, Decreased dendritic spine density on prefrontal cortical pyramidal neurons in schizophrenia. *Archives of General Psychiatry* **57**, 65-73 (2000).

56. L. D. Selemon, G. Rajkowska, P. S. Goldman-Rakic, Abnormally high neuronal density in the schizophrenic cortex. A morphometric analysis of prefrontal area 9 and occipital area 17. *Archives of General Psychiatry* **52**, 805-818 (1995).

57. K. J. Brennand *et al.*, Modeling schizophrenia using human induced pluripotent stem cells. *Nature* **473**, 211-225 (2011).

58. K. J. Brennand *et al.*, Phenotypic differences in hiPSC NPCs derived from patients with schizophrenia. *Molecular Psychiatry* **20**, 361–368 (2015).

59. Y. Yang *et al.*, Enhanced rejuvenation in induced pluripotent stem cell-derived neurons compared with directly converted neurons from an aged mouse. *Stem Cells and Development* **00**, (2015).

60. E. Dantuma, S. Merchant, K. Sugaya, Stem cells for the treatment of neurodegenerative diseases. *Stem Cell Research and Therapy* **1**, (2010).

61. K. Hochedlinger, K. Plath, Epigenetic reprogramming and induced pluripotency. *Development* **136**, 509-523 (2009).

62. C. H. Chiang *et al.*, Integration-free induced pluripotent stem cells derived from schizophrenia patients with DISC1. *Molecular Psychiatry* **16**, 358-360 (2001).

63. E. Pedrosa *et al.*, Development of patient-specific neurons in schizophrenia using induced pluripotent stem cells. *Journal of Neurogenetics* **25**, 88-103 (2011).

64. S. Anand, K. Sugaya, Stem cell approaches for treatment of neurodegenerative diseases. *Clinical Pharmacology & Biopharmaceutics* **3**, (2014).

65. H. Stefansson *et al.*, *Neuregulin 1* and susceptibility to schizophrenia. *The American Journal of Human Genetics* **71**, 877-892 (2002).

66. S. J. Glatt, S. V. Faraone, M. T. Tsuang, Association between a functional Catechol *O*-Methyltransferase gene polymorphism and schizophrenia: meta-analysis of case-control and family-based studies. *American Journal of Psychiatry* **160**, 469-476 (2003).

67. T. Li *et al.*, Identification of a novel neuregulin 1 at-risk haplotype in Han schizophrenia Chinese patients, but no association with the Icelandic/Scottish risk haplotype. *Molecular Psychiatry* **9**, 698-704 (2004).

68. D. L. Braff, R. Freedman, N. J. Schork, I. I. Gottesman, Deconstructing schizophrenia: an overview of the use of endophenotypes in order to understand a complex disorder. *Schizophrenia Bulletin* **33**, 21-32 (2007).

69. T. L. Young-Pearse, S. Suth, E. S. Luth, A. Sawa, D. J. Selkoe, Biochemical and functional interaction of disrupted-in-schizophrenia 1 and amyloid precursor protein regulates neuronal migration during mammalian cortical development. *Journal of Neuroscience* **30**, 10431-10440 (2010).

70. L. E. Duncan *et al.*, Pathway analyses implicate glial cells in schizophrenia. *POLS ONE* **9**, (2014).

71. M. Maschietto *et al.*, Co-expression network of neural-differentiation gene shows specific pattern in schizophrenia. *BMC Medical Genomics* **8**, (2015).

72. T. Morimura, M. Ogawa, Relative importance of the tyrosine phosphorylation sites of Disabled-2 to the transmission of Reelin signaling. *Brain Research* **1304**, 26-37 (2009).